Transceiver Design for MIMO DCO-OFDM in Visible Light Communication

Jian Dang, Mengting Wu, Liang Wu and Zaichen Zhang

Additional information is available at the end of the chapter

Abstract

Direct current-biased optical-orthogonal frequency-division multiplexing (DCO-OFDM) is a simple yet spectrally efficient multicarrier modulation scheme for visible light communication (VLC). But in multiple-input multiple-output (MIMO) scenario, which is more practical for VLC due to the LED deployment, the research on DCO-OFDM is still limited and calls for in-depth investigation. In this chapter, we first study the basic modulation scheme of DCO-OFDM, including the design of conventional receiver without considering the clipping noise. Secondly, we present a novel receiver for combating clipping distortion in the DCO-OFDM system, which can reconstruct the clipping noise and subtract it from the received signal. Thirdly, we generalize the results to MIMO scenario and investigate the preliminary transceiver design, which is based on the minimum mean-square error (MMSE) criteria. Based on this, we propose a precoding algorithm to further enhance the performance. Finally, the symbol error rate performance is compared through computer simulations to give the reader a whole picture of the performance of MIMO VLC system.

Keywords: clipping noise, DCO-OFDM, iterative reconstruction, transceiver design, DCO-OFDM

1. Introduction

As an important complementary technique to the fifth generation (5G) wireless communication system, visible light communication (VLC) is currently enjoying a promising development in the research area of communication [1]. VLC transmits information with the visible light emitted by the light emitting diodes (LEDs), which are generally deployed to provide indoor

INTECH
open science | open minds

illumination simultaneously. In VLC, simple low-cost intensity modulation and direct detection (IM/DD) techniques are employed to send information, which implies that the phase cannot be used to convey any information. Therefore, pulsed modulation schemes such as pulse position modulation (PPM), pulse width modulation (PWM) or on-off keying (OOK) is employed in practical VLC systems [2].

In order to combat the inter-symbol interference caused by the indoor optical wireless channel, orthogonal frequency-division multiplexing (OFDM) has been considered for VLC due to its inherent robustness to multipath effect [3]. In VLC, the transmitted electrical signal is used to modulate the light intensity of the LED. For this purpose, the transmitted electrical signal must be real and non-negative. Therefore, the traditional OFDM needs to be modified to obtain the real-valued signal, which can be produced by imposing Hermitian symmetry symbols on the frequency domain subcarriers and then conducting inverse discrete Fourier transform (IDFT) operation on these frequency domain subcarriers. In general, there are two approaches to obtain non-negative signal from the above real-valued signal. One approach is asymmetrically clipped optical OFDM (ACO-OFDM) which is proposed in Ref. [4]. The other approach is the direct current (DC)-biased optical (DCO-OFDM), which is more spectrally efficient than ACO-OFDM [5]. The differences between ACO-OFDM and DCO-OFDM are explained in more detail in Refs. [5, 6].

One major problem of OFDM modulation is its high peak-to-average power ratio (PAPR), which results from the summation over a large number of subcarriers. Therefore, the time domain DCO-OFDM signal often has to be double-sided clipped to fit the dynamic linear range of the transmitter, which inevitably introduces clipping distortion [7]. Although some papers have analysed the double-sided clipped DCO-OFDM, to our knowledge, few of them focus on improving the performance of the receiver [8]. In Ref. [9], the authors only analysed the performance of the double-sided clipped DCO-OFDM in terms of the achievable data rate and error vector magnitude. In Ref. [8], an optimum DC bias method has been proposed for the double-sided clipped DCO-OFDM in order to decrease the clipping effects of the transmitter. In Refs. [3–9], only the conventional receiver is utilized in DCO-OFDM. The conventional receiver for DCO-OFDM usually does not care for the clipping noise and only simply subtracts the DC bias from the received signal in the process of demodulation. Not surprisingly, it can only provide suboptimal performance, especially in heavily clipped scenarios. In this chapter, we are interested in designing the high-performance receiver for DCO-OFDM. First, we analyse the structure of the transmitted signal. Then, the clipping noise can be modelled as a certain signal format that is based on the lower and upper clipping bounds. At last, we propose a new receiver for DCO-OFDM, which reconstructs the clipping noise and decodes data in an iterative manner by exploiting the signal structure of the clipping noise. The complexity of the new receiver is comparable with the conventional one. Moreover, the convergence rate of the new receiver is very fast, about 2–5 iterations. Therefore, the proposed receiver can provide a realistic implementation in the DCO-OFDM system. Simulation results demonstrate the large performance gains compared to the conventional receiver.

On the other aspect, the low-cost white LED has limited modulation bandwidth, which prohibits high transmission rate of VLC, and optical multiple-input multiple-output (MIMO) can

help achieve high data rate by utilizing spatial diversity [10]. Therefore, OFDM can also be deployed together with MIMO in VLC systems to further enhance the bandwidth utilization efficiency and boost the data rates [11, 12]. Some experimental results have demonstrated that high data rates up to gigabit/s can be achieved in the MIMO VLC system [12]. In this chapter, we first describe a MIMO VLC system, which can effectively support the flickering/dimming control and other lighting requirements [13]. Secondly, in order to drive an LED transmitter, we illustrate how the dynamic range constraint and dimming control impact the design of MIMO transceiver [14]. Finally, an advanced method on MIMO transceiver design is proposed and studied by theoretical analysis and simulation. It turns out that the bit error rate (BER) performance of the MIMO VLC system could be improved by the advanced joint optimization method.

For convenience, we summarize the mathematical notations here. Bold and lowercase symbols (e.g. $\boldsymbol{a}$) denote column vectors. Specifically, $\boldsymbol{1}$ denotes a column vector whose elements are 1. Bold and uppercase symbols (e.g. $\boldsymbol{H}$) denote matrices. Specifically, $\boldsymbol{W}_N$ denotes the N × N DFT matrix. The superscripts $(\cdot)^*$, $(\cdot)^T$, $(\cdot)^H$ and $(\cdot)^{-1}$ denote the complex conjugate, transpose, conjugate transpose and inverse of a matrix/vector, respectively. sign(a) returns the signs of a (here 0 is replaced by 1), $E\{\cdot\}$ denotes the statistical expectation, diag($\cdot$) is a diagonal matrix whose entries on the main diagonal are given by a matrix, Tr($\cdot$) is the trace of a matrix, $\|\cdot\|$ denotes the Frobenius norm, min($\cdot$) denotes an element-wise minimum operator and abs($\cdot$) denotes an element-wise absolute operator.

2. Conventional receiver for DCO-OFDM

2.1. System model of DCO-OFDM

The DCO-OFDM system model considered in this chapter is shown in **Figure 1**. At the transmitter, the source bits $\boldsymbol{b}$ (coded or uncoded) are first modulated using M-ary square quadrature amplitude modulation (QAM) to get the complex signal $\boldsymbol{X}$. In order to get the real output of time domain OFDM signal after IDFT operation, the input frequency domain vector $\tilde{\boldsymbol{X}}$ of the IDFT module must be symmetrically conjugated, which requires Hermitian symmetric expansion of $\boldsymbol{X}$. The specific expansion is given as follows:

$$\boldsymbol{X} = \left[X(0), X(1), ..., X\left(\frac{N}{2} - 1\right) \right]^T, X(0) = 0, \tag{1}$$

$$\tilde{\boldsymbol{X}} = [\tilde{X}(0), \tilde{X}(1), ..., \tilde{X}(N-1)]^T, \tag{2}$$

$$\tilde{X}(k) = \begin{cases} X(K), & 0 \leq k \leq \dfrac{N}{2} - 1 \\ 0, & k = \dfrac{N}{2} \\ X^*(n-k), & \dfrac{N}{2} + 1 \leq k \leq N - 1 \end{cases}. \tag{3}$$
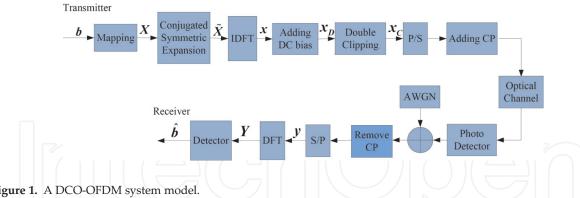
Figure 1. A DCO-OFDM system model.

Here, $\tilde{X}(0)$ and $\tilde{X}(N/2)$ do not carry information and are generally set to zeros. Thus, the number of unique data carrying subcarriers present is $\frac{N}{2} - 1$. Then, the discrete time-domain real-valued OFDM signal x is generated by applying IDFT operation to $\tilde{X}$ as

$$x(n) = \frac{1}{\sqrt{N}} \sum_{k=0}^{N-1} \tilde{X}(k) \exp\left(\frac{j2\pi kn}{N}\right), n = 0, 1, \ldots, N-1, \tag{4}$$

where $j = \sqrt{-1}$ and N is the size of IDFT. When N is not very small, according to the central limit theorem, it is reasonable to model x as an independent identical distributed (i.i.d) Gaussian vector with zero mean. In order to drive the LED and fit the dynamic linear range of the transmitter simultaneously, the signal should be added with a proper DC bias, which leads to x_D as

$$x_D = x + \mathbf{1} \cdot D, \tag{5}$$

where D is the DC bias. In DCO-OFDM, double-sided clipping should be applied to x_D to fit the dynamic linear range of the LED. Then, x_D needs to be clipped at both lower and upper bounds to get x_C, which can be described as

$$x_C(n) = \begin{cases} C_L, & x_D(n) < C_L \\ x_D(n), & C_L \le x_D(n) \le C_U \\ C_U, & x_D(n) > C_U \end{cases} \tag{6}$$

where C_L and C_U are the lower and upper clipping bounds, respectively, which need to satisfy the constraint of $C_L \le x_D(n) < C_U$. We note that Eq. (6) can be rewritten as

$$x_C(n) = x(n)f_1\big(x(n)\big) + D \cdot f_1\big(x(n)\big) + C_L \cdot f_2\big(x(n)\big) + C_U \cdot f_3\big(x(n)\big) \tag{7}$$

by defining

$$f_1\big(x(n)\big) = \frac{sign\big(x(n) + D - C_L\big) + 1}{2} \cdot \frac{sign\big(C_U - x(n) - D\big) + 1}{2}, \tag{8}$$

$$f_2\big(x(n)\big) = \frac{sign\big(C_L - x(n) - D\big) + 1}{2}, \tag{9}$$

$$f_3\big(x(n)\big) = \frac{sign\big(x(n) + D - C_U\big) + 1}{2}. \tag{10}$$

In vector form:

$$x_C = F_1 x + f_1 \cdot D + f_2 \cdot C_L + f_3 \cdot C_U, \tag{11}$$

$$F_1 = diag(f_1) = diag\big(f_1\big(x(0)\big), f_1\big(x(1)\big), ..., f_1\big(x(N-1)\big)\big). \tag{12}$$

At the transmitter, x_C is appended with the cyclic prefix (CP) to avoid inter-symbol interference and then drives the LED.

The optical signal from the LED spreads through the optical channel and then arrives at the receiver, where a photodetector (PD) can retrieve the electrical signal on the basis of the intensity of the received optical signal. After removing CP, the received signal in time domain and frequency domain after DFT is denoted as y and Y, respectively. In VLC, the equivalent electrical domain channel between x_C and y is denoted by h, which may be a direct path and/or reflected paths. All the components of h are real and non-negative. The frequency domain channel of h is denoted as H, and we define $H = diag(H)$, which is based on the principles of OFDM system and the singular value decomposition (SVD) of circle matric. The received signal in the frequency domain can be expressed as

$$Y = HX_C + Z \tag{13}$$

where $X_C = W_N x_C$ and Z is the additive white Gaussian noise in the frequency domain and each of its sample has zero mean and variance σ^2. To facilitate the derivation of the new receiver in subsection III, we rewrite Eq. (13) by combining Eqs. (7)–(12) as

$$\begin{aligned} Y &= HW_N(F_1 x + f_1 \cdot D + f_2 \cdot C_L + f_3 \cdot C_U) + Z \\ &= HW_N F_1 W_N^H X + HW_N f_1 \cdot D + HW_N f_2 \cdot C_L + HW_N f_3 \cdot C_U + Z. \end{aligned} \tag{14}$$

It is worth noting that DC bias D should be carefully designed to reduce distorting the signal x as little as possible [8], which is beyond the scope of this chapter.

2.2. Conventional receiver design of DCO-OFDM

For the conventional receiver, it does not care for the clipping noise, that is, it models x_C as follows:

$$x_C \approx x_D = x + 1 \cdot D. \tag{15}$$

Thus, the received signal in the frequency domain is

$$Y \approx HW_N(x + 1 \cdot D) + Z = H\tilde{X} + HW_N 1 \cdot D + Z. \tag{16}$$

At the receiver, the DC bias is first removed by

$$Y_1 = Y - HW_N\mathbf{1} \cdot D \approx H\tilde{X} + Z. \tag{17}$$

Then, based on Eq. (17), the receiver can decode the data. This is a common estimation problem in wireless communications and there are many available estimation methods. Without loss of generality, in this chapter, we select the linear minimum mean-square error (LMMSE) estimator because of its good complexity-performance trade-off. The estimate of $\tilde{X}$ is given by

$$\tilde{X}_{\mathrm{conv}} = (H^H H + \sigma^2 I_{\mathrm{N}})^{-1} H^H Y_1 \tag{18}$$

3. Advanced receiver for DCO-OFDM

3.1. Advanced receiver design of DCO-OFDM

While the conventional receiver is simple to implement, it does not suppress the clipping noise in the process of demodulation, which inevitably degrades the system performance severely, especially in a heavily clipped case. Here, we propose a novel receiver, which iteratively reconstructs the clipping noise using the structure of the clipping noise and subtracts it from the received signal. Then, one can get the signal with less clipping noise. Subsequently, we conduct the LMMSE on the signal with less chipping noise to obtain the more accurately detected source bits $\hat{b}$. Based on Eq. (14), the clipping noise is given as

$$Z_{\mathrm{C}} = HW_N f_1 \cdot D + HW_N f_2 \cdot C_L + HW_N f_3 \cdot C_U. \tag{19}$$

Here in Eq. (19), reconstructing Z_C is dependent on the data $\tilde{X}$ since f_1, f_2 and f_3 are functions of x. Therefore, we propose the following iterative algorithm to decode the data.

Algorithm 1: Proposed iterative for DCO-OFDM

Step 1. Initialization:

Using the conventional receiver that is based on Eq. (18), obtain the estimation of $\tilde{X}$, denoted by $\tilde{X}_{\mathrm{conv}}$. Then, reconstruct the time domain signal $\hat{x}$ which is an approximation of x by performing IDFT operation on $\tilde{X}_{\mathrm{conv}}$.

Step 2. Iteration:

1. Based on Eqs. (8)–(10) and $\hat{x}$, obtain the estimated values of f_1, f_2 and f_3;

2. Based on Eq. (19), construct the estimated clipping noise $\tilde{Z}_C$, and then subtract $\tilde{Z}_C$ from the received frequency domain signal Y to get the estimate of

$$Y_{sci} = Y - \tilde{Z}_C \approx HW_N F_1 W_N^H X + Z. $$

3. If F_1 is full rank, go to (4) or otherwise go to (5).

4. Perform LMMSE on Y_{sci} to obtain $\tilde{X}_{prop}$, which is an updated estimation of $\tilde{X}$. Then, construct $\hat{x}$ based on $\tilde{X}_{prop}$ by performing IDFT operation;

5. Based on $W_N^H H^{-1} Y_{sci} \approx F_1 x + W^H H^{-1} Z$, or $y_{sci} \approx F_1 x + z_{sic}$, if $F_1(n, n) = 0$, replace $y_{sic}(n)$ with the former estimation of $x(n)$. Through the updated y_{sci}, obtain $\tilde{X}_{prop}$, and then construct $\hat{x}$.;

6. If the algorithm has reached a predefined number of iterations, go to (3) or otherwise go to (1).

Step 3. Demapping:

Extract $\tilde{X}_{prop}$ with indices 1, 2, …, $N/2 - 1$ and then perform demapping to get the source bit estimates $\hat{b}$.
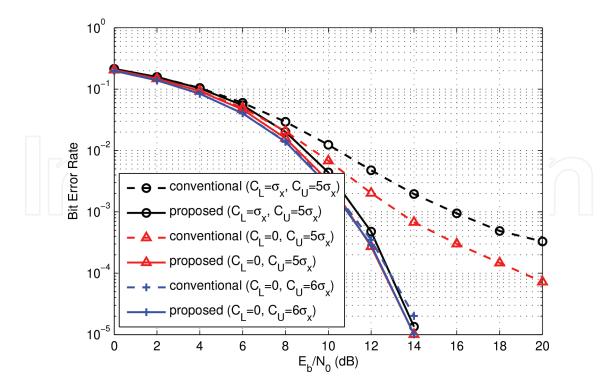
In the following, we address some issues in the process of implementing the proposed receiver that one should pay attention to.

1. $f_1(\cdot)$ is 0,which corresponds to the negative clipping effects. Thus, F_1 cannot be inverted. Therefore, if we suppose that $HW_N F_1 W_N^H$ could be inverted, using $Y_{sci} = Y - \tilde{Z}_C \approx HW_N F_1 W_N^H X + Z$ with LMMSE will result in bad performance.

2. To get rid of the inversion of F_1, we use the following methods: $W_N^H H^{-1} Y_{sci} \approx F_1 x + W^H H^{-1} Z$ or $y_{sci} \approx F_1 x + z_{sic}$. If $F_1(n, n) = 0$; then no information could be obtained for $x(n)$ from $y_{sic}(n)$; thus, we use former estimation of $x(n)$ If $F_1(n, n) = 1$, then $x(n)$ could be reestimated by $y_{sic}(n)$. After all, $x(n)$ is obtained and $\tilde{X}$ could be obtained.
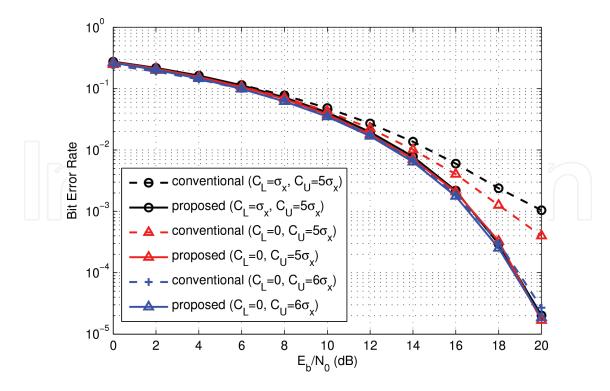
3.2. Numerical results of DCO-OFDM

In this section, we show numerical results of the average uncoded BER performance for the proposed receiver under different double-sided clipping bounds and different modulation sizes of QAM and compare it with the conventional receiver. The channels are generated using the method in Ref. [2] with the following parameters: an empty room of size 8 m × 6 m × 4 m, the reflection coefficients for the ceiling, the wall and the floor which are 0.8, 0.8 and 0.3, respectively and the LED is attached 0.1 m below the ceiling and the photodetector is 1 m above the floor with an 80 degree of field of view (FOV). The LED pointing straight downward and upward can generate line-of-sight (LOS) and non-line-of-sight (NLOS) channels, respectively. The channels are normalized to have the power 1. The transmit power of x is normalized to 1, that is $\sigma_x = 1$. The upper and lower clipping bounds are set to be linearly proportional to σ_x. The number of subcarriers is $N = 64$. The DC bias is set to be $3\sigma_x$.
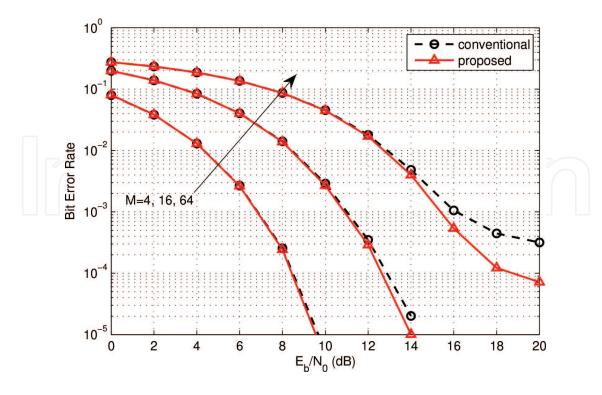
Figures 2 and **3** present the BER performance with the different double-sided clipping bounds and the fixed modulation size $M = 16$, in LOS and NLOS channels, respectively. **Figure 4** shows the BER performance with the different modulation sizes and the fixed double-sided clipping bound ($C_L = 0$, $C_U = 6\sigma_x$) in LOS channels. **Figure 5** presents the BER performance with the different modulation sizes and the fixed double-sided clipping bound ($C_L = 0$, $C_U = 5\sigma_x$) in NLOS channels. Through simulations, it is observed that the proposed receiver converges after only 2 iterations for most times. Therefore, 2 iterations are involved for the proposed receiver.
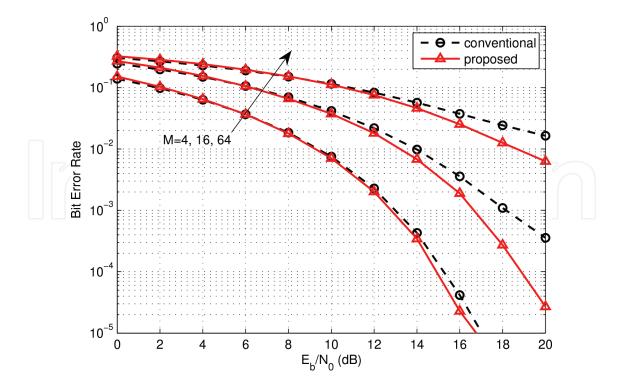
Figure 2. BER comparison between the proposed receiver and the conventional receiver with different lower and upper clipping bounds and fixed modulation size $M = 16$ in LOS channels.

Figure 3. BER comparison between the proposed receiver and the conventional receiver with different lower and upper clipping bounds and fixed modulation size $M = 16$ in NLOS channels.

Figure 4. BER comparison between the proposed receiver and the conventional receiver with different modulation sizes and the fixed lower and upper clipping bounds ($C_L = 0$, $C_U = 6\sigma_x$) in LOS channels.



Figure 5. BER comparison between the proposed receiver and the conventional receiver with different modulation sizes and the fixed lower and upper clipping bounds ($C_L = 0$, $C_U = 5\sigma_x$) in NLOS channels.

We can obtain several facts from **Figures 2–5**. First, the proposed receiver outperforms the conventional one in any case, that is, in both LOS and NLOS and with different double-sided clipping bounds and different modulation sizes. Second, the signal noise ratio (SNR) gain over the conventional receiver could be much more than 3 dB, especially when decreasing the clipping range. Although the SNR gain over the conventional receiver could fade away when increasing the clipping range, the larger clipping range requires the larger dynamic linear range of the LED, which is difficult to satisfy in practice. Finally, the proposed receiver can give better performance when higher order QAM formats are employed. Therefore, the proposed receiver can provide better performance than the conventional receiver.

4. Transceiver design for MIMO DCO-OFDM

In the field of MIMO VLC system, the joint design of precoder and equalizer still need deep research. In previous works, a simple way to design the transceiver in MIMO VLC systems was to apply the channel matrix inversion at the receiver side [12]. If the channel matrix is rank-deficient or not squared, pseudo-inversion operation is used instead. However, these methods might result in noise amplification if the values of elements in the channel matrix were low [15]. In Refs. [13, 14], a MIMO VLC system was proposed, which can effectively support the flickering/dimming control and other lighting requirements. Moreover, in such a system, the precoder and equalizer can be adaptively optimized according to different input signals and various illumination levels. Based on Ref. [14], we propose an advanced transceiver design on MIMO VLC systems, which will be detailed in this section.

4.1. System model of MIMO DCO-OFDM

A MIMO DCO-OFDM system for optical wireless communication is surveyed and simulated in Ref. [16], and from this research, it is known that an MIMO DCO-OFDM system can be equivalently split into N parallel MIMO subsystems with single-tap channels in the frequency domain, where N is the number of subcarriers. Therefore, for simplicity and without loss of generality, we only investigate a specific subcarrier of the MIMO DCO-OFDM system which can be modelled as a single-path MIMO subsystem. The result can be readily extended to the whole MIMO DCO-OFDM system. **Figure 6** shows the simplified MIMO subsystem with N_t LEDs at the transmitter and N_r photodetectors at the receiver. The optical MIMO channel is
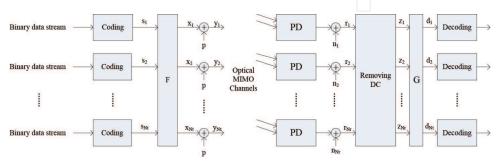

Figure 6. The simplified MIMO DCO-OFDM system model.

modelled as an $N_t \times N_r$ matrix, whose element h_{mn} is real-valued and represents the channel gain between the nth LED and the mth PD.

Here, we assume that the channel response in each transmission period is flat, and the multi-level pulse amplitude modulation (PAM) is a practical example for this section. Moreover, PPM or PWM is not considered here because different pulse positions and various pulse widths (caused by dimming control) from different LEDs can make MIMO detection more complicated than the case of PAM. Since VLC employs IM/DD technology, the signals must be real-valued. Thus, all vectors and matrices are real-valued in this chapter.

4.1.1. Transmitter side

From **Figure 6**, we know that N_t binary data streams are firstly modulated into the source data vector $s(\tau) = [s_1(\tau), ..., s_{N_t}(\tau)]^T$ For convenience, we ignore the time index τ in the rest of this chapter. Taking into account the actual situation, we assume that the source data s_k is zero mean and bounded as

$$-b_k \leq s_k \leq b_k. \tag{20}$$

Because of the characteristics of the optical channel, the source data streams cannot drive the LEDs directly. To meet dimming control and the dynamic-range constraints of LEDs, the source data vector will be multiplied by an $N_t \times N_r$ precoder matrix F and then added by the DC biasing $p = p \times 1$, which is shown in **Figure 6**. Such a MIMO VLC transmitter structure was firstly introduced in Ref. [13] but only the real-valued LED transmission signals were considered.

The transmitted signal can be expressed as $y = Fs + p$, where we assume that the LED electrical-to-optical conversion is linearized [17] and the overall gain is chosen as 1 for convenience without loss of generality. For each LED, we assume that $[l, u]$ $(0 < l)$ is the dynamic-range constraint, and in order to meet the dimming control, we should have

$$0 < l \leq y_i = \sum_{k=1}^{N_t} f_{ik} s_k + p \leq u. \tag{21}$$

Combining with Eq. (20), we know that the signal after precoder satisfies

$$-\sum_{k=1}^{N_t} |f_{ik}| b_k \leq \sum_{k=1}^{N_t} f_{ik} s_k \leq \sum_{k=1}^{N_t} |f_{ik}| b_k. \tag{22}$$

So, we need

$$\sum_{k=1}^{N_t} |f_{ik}| b_k \leq u - p, \tag{23}$$

$$\sum_{k=1}^{N_t} |f_{ik}| b_k \leq p - l, \tag{24}$$

to meet the brightness control of LEDs, and we can rewrite Eqs. (23) and (24) as

$$abs(\boldsymbol{F})\boldsymbol{b} \le min\{\boldsymbol{u} - \boldsymbol{p}, \boldsymbol{p} - \boldsymbol{l}\}, \tag{25}$$

where $\boldsymbol{u} = u \times \boldsymbol{1}$, $\boldsymbol{l} = l \times \boldsymbol{1}$. The DC bias vector can affect the performance of precoder and equalizer, and from Ref. [13], we can know that the BER performance is best when the DC bias is the midpoint of l and u. That is, when $p = \frac{1}{2}(l + u)$, we can get a high-performance precoder and equalizer under the constraint of Eq. (25).

4.1.2. Receiver side

From **Figure 6**, we know that N_r PDs are used to convert the optical signals to electrical signals at receiver. The received signals can be expressed as

$$\boldsymbol{r} = \boldsymbol{H}\boldsymbol{y} + \boldsymbol{n} = \boldsymbol{H}(\boldsymbol{F}\boldsymbol{s} + \boldsymbol{p}) + \boldsymbol{n}, \tag{26}$$

where $\boldsymbol{n}$ is the additive white Gaussian noise (AWGN) with zero mean and independent of the data. That is, all the noise components are independently identically distributed. After removing DC components, the signal can be represented by

$$\boldsymbol{z} = \boldsymbol{r} - \boldsymbol{H}\boldsymbol{p} = \boldsymbol{H}\boldsymbol{F}\boldsymbol{s} + \boldsymbol{n}, \tag{27}$$

and a linear equalizer is used to recover the source data, which is shown as

$$\boldsymbol{d} = \boldsymbol{G}\boldsymbol{z} = \boldsymbol{G}\boldsymbol{H}\boldsymbol{F}\boldsymbol{s} + \boldsymbol{G}\boldsymbol{n}. \tag{28}$$

Finally, after the decoding part, the source signal is demodulated from $\boldsymbol{d}$. There are some detection methods to estimate the source data, and we utilize the MMSE criterion:

$$\tilde{\boldsymbol{s}} = \arg\min_{\boldsymbol{s} \in S}\|\boldsymbol{d} - \boldsymbol{s}\|^2, \tag{29}$$

where S is the set of all possible source data vectors.

4.2. Transceiver design of MIMO DCO-OFDM

In this section, we focus on designing the MIMO transceiver with the knowledge of the channel state information (CSI), which means, given the channel matrix $\boldsymbol{H}$, we should determine the procoder matrix $\boldsymbol{F}$ and the equalizer matrix $\boldsymbol{G}$.

4.2.1. Iterative MMSE transceiver

In order to recover the source data from the received signal, we can formulate the problem below: design the procoder matrix $\boldsymbol{F}$ at the transmitter and the equalizer matrix $\boldsymbol{G}$ at the receiver to minimize the MSE between the transmitted data and the recovered data, that is,

$$\min_{F, G} MSE(\boldsymbol{d}, \boldsymbol{s}, \boldsymbol{F}, \boldsymbol{G})$$
$$\text{s.t. } \text{abs}(\boldsymbol{F})\boldsymbol{b} \leq \min\{\boldsymbol{u} - \boldsymbol{p}, \boldsymbol{p} - \boldsymbol{l}\} \ . \tag{30}$$

Given the channel matrix $\boldsymbol{H}$, we have

$$
\begin{aligned}
MSE(\boldsymbol{d}, \boldsymbol{s}, \boldsymbol{F}, \boldsymbol{G}) &= \mathrm{E}\{\|\boldsymbol{d} - \boldsymbol{s}\|^2\} = \mathrm{E}\{\|\boldsymbol{GHFs} + \boldsymbol{Gn} - \boldsymbol{s}\|^2\} \\
&= \mathrm{E}\Big\{Tr\{(\boldsymbol{GHFs} + \boldsymbol{Gn} - \boldsymbol{s})(\boldsymbol{GHFs} + \boldsymbol{Gn} - \boldsymbol{s})^H\}\Big\} \\
&= \mathrm{E}\Big\{Tr\{[(\boldsymbol{GHF} - \boldsymbol{I})\boldsymbol{s} + \boldsymbol{Gn}][\boldsymbol{s}^H(\boldsymbol{GHF} - \boldsymbol{I})^H + \boldsymbol{n}^H\boldsymbol{G}^H]\}\Big\} \\
&= Tr\{\boldsymbol{GHFR_sF}^H\boldsymbol{H}^H\boldsymbol{G}^H\} + Tr\{\boldsymbol{GR_nG}^H\} + Tr\{\boldsymbol{R_s}\} - Tr\{\boldsymbol{GHFR_s}\} - Tr\{\boldsymbol{R_sF}^H\boldsymbol{H}^H\boldsymbol{G}^H\},
\end{aligned}
\tag{31}
$$

where $\boldsymbol{R_s} = \mathrm{E}\{\boldsymbol{ss}^H\}$, $\boldsymbol{R_n} = \mathrm{E}\{\boldsymbol{nn}^H\}$. In this chapter, we assume that the source data is independent of the noise. Combining Eq. (30) with Eq. (31), an iterative algorithm was developed in [13, 14], which is briefly shown in next two steps:

1. Updating $\boldsymbol{G}$ as $\boldsymbol{F}$ is given:

    Given $\boldsymbol{F}$, by setting $\frac{\partial MSE(\boldsymbol{d}, \boldsymbol{s}, \boldsymbol{F}, \boldsymbol{G})}{\partial \boldsymbol{G}} = 0$, we have the MMSE equalizer:

    $$\boldsymbol{G} = \boldsymbol{R_sF}^H\boldsymbol{H}^H(\boldsymbol{HFR_sF}^H\boldsymbol{H}^H + \boldsymbol{R_n})^{-1}. \tag{32}$$

2. Updating $\boldsymbol{F}$ as $\boldsymbol{G}$ is given:

    Given $\boldsymbol{G}$, we can update $\boldsymbol{F}$ by minimum Eq. (31), which is linear and contains the element-wise absolute operator, and it is difficult to use the traditional optimization algorithm to get $\boldsymbol{F}$. With the help of matrix multiplication knowledge [18], the objective function of Eq. (31) can be rewritten as

$$\min_F MSE(\boldsymbol{d}, \boldsymbol{s}, \boldsymbol{F}, \boldsymbol{G}) = \min_F \mathrm{vec}(\boldsymbol{F}^H)^H((\boldsymbol{H}^H\boldsymbol{G}^H\boldsymbol{GH}) \otimes \boldsymbol{R_s})\mathrm{vec}(\boldsymbol{F}^H) - 2\mathrm{vec}(\boldsymbol{F}^H)^H\mathrm{vec}(\boldsymbol{R_sGH}). \tag{33}$$

So far, the original optimization problem can be transformed into a convex linearly constrained quadratic programme (LCQP) problem, which can be solved by a software package for convex programmes called CVX [13]. Through simulations, it is observed that the iterative MMSE transceiver converges after only five iterations for most times. Therefore, five iterations are involved for the iterative MMSE transceiver.

4.2.2. Advanced MMSE transceiver

The iterative MMSE transceiver presented in the previous section is a quite smart method to design the MIMO transceiver, which can effectively support the dimming control, dynamic-range constraint and other VLC-specific requirements. However, we find that the boundary condition of Eq. (25) is too harsh for practical applications, which can lead to a waste of illumination bandwidth. Thus, we propose a coefficient r to enlarge $\boldsymbol{F}$, that is,

$$F_{adv} = F_{ite} * r, \tag{34}$$

where F_{ite} is the precoder we get from the iterative MMSE transceiver [14] and F_{adv} is the advanced precoder. With r, the elements of F_{adv} make any signal that satisfies

$$\max_{1 \le i \le N_t} \left| \sum_{k=1}^{N_t} f_{ik} s_k \right| = \min\{p - l, u - p\}, \tag{35}$$

which improves the BER performance of MIMO transceiver in practical VLC systems.

Algorithm 2: Advanced algorithm for joint design of F and G

Step 1. Initialization:

1.   Estimate channel matrix H and noise parameter R_n;

2.   Set illumination constraint $[l, u]$ and modulation scheme (b and F_s).

3.   Initialize precoder matrix F_0 within the constraint of Eq. (25), for example, $F_0 = tI_{N_t}$, where $0 < t \le \min_{1 \le k \le N_t} \left\{ \frac{u-p}{b_k}, \frac{p-l}{b_k} \right\}$.

Step 2. Iteration:

1.   Update G_i with given F_{i-1} by using Eq. (32).

2.   With G_i, rewrite objective function Eq. (33) and figure out optimal F_i by CVX.

3. $i = i + 1$.

Step 3. Termination:

$\frac{\|F_i - F_{i-1}\|^2}{\|F_{i-1}\|^2} \le 10^{-3}$, where 10^{-3} is the predefined threshold or $i = 50$, where 50 is the predefined default max iteration number.

Step 4. Application:

1.   Use F_{ite} that we get from Step 3 and Eq. (35); then we can obtain r and F_{adv};

2.   Update G_{adv} with F_{adv} again by using Eq. (32).

3.   Apply F_{adv} and G_{adv} as MIMO transceivers in practical VLC systems.

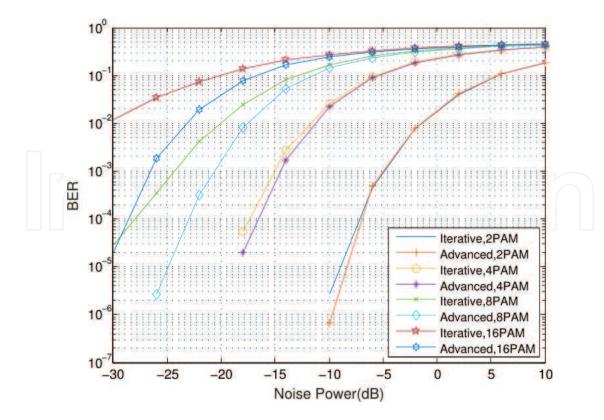### 4.3. Numerical results of MIMO DCO-OFDM

Here, we assume the channels are flat for simplicity but the results could be extended to frequency-selective channels with proper modifications. In the previous sections, we have performed theoretical analysis of the optimal transceiver design for the MIMO VLC systems, and the advanced iterative MMSE transceiver can be easily implemented into the practical design of the procoder and equalizer. In this section, we would like to show some simulation results to verify the proposed MIMO VLC system and the advanced iterative MMSE algorithm. Through simulations, it is observed that the advanced MMSE transceiver converges after only 5 iterations for most times, which is the same as the iterative MMSE transceiver. In the advanced

MMSE transceiver, the number of iterations is no more than M, and in each iteration, a matrix inversion and a CVX operation are needed to be done so the total complexity of the proposed algorithm is $O(MN_t^3) + O(Q)$, and $0(Q)$ is the complexity of the CVX operation.

In the simulation, we consider a 5×5 MIMO VLC system and we choose the channel matric as

$$H = \begin{bmatrix} 0.6386 & 0.0483 & 0.7141 & 0.4211 & 0.1484 \\ 0.4979 & 0.7962 & 0.0981 & 0.9548 & 0.0805 \\ 0.9216 & 0.9709 & 0.9140 & 0.1895 & 0.7115 \\ 0.3472 & 0.7417 & 0.7847 & 0.2734 & 0.0700 \\ 0.0221 & 0.2788 & 0.1518 & 0.0538 & 0.5241 \end{bmatrix}$$; the dimming control of LEDs is

selected as $l=1$ and $u=9$. We assume the signals and the noise are independently identically distributed; then, we have $\mathbf{R}_s = \sigma_s^2 \mathbf{I}_5$ and $\mathbf{R}_n = \sigma_n^2 \mathbf{I}_5$. Because the precoder will adaptively adjust the transmitted signal power, we set $\sigma_s^2 = 1$. Additionally, 2-PAM/4-PAM/8-PAM/16-PAM are used, thus, $b_k = 1/\frac{3}{\sqrt{5}}/\frac{7}{\sqrt{21}}/\frac{15}{\sqrt{85}}$ (power normalization, e.g. $\sigma_s^2 = 1$). From Ref. [13], we choose $p = \frac{1}{2}(l+u) = 5$, and we can get a high-performance precoder and equalizer under the constraint of Eq. (25). For the SNR consideration, the noise power is selected from the range $[-30, 10]$ dBm.

Two different MIMO schemes are compared in our simulations: the first scheme utilizes the MMSE precoder and equalizer derived from the iterative algorithm in Section 5.2.1. In the second scheme, the advanced MMSE precoder and equalizer derived from the algorithm 2 are used. Moreover, we take into consideration the impact of dimming control and BER that is simulated as the metric to evaluate the performance. The simulation results of the BER performance of the different transceivers with various noise levels in MIMO VLC systems are shown in **Figure 7**.

Figure 7. BER performance of the iterative MMSE transceivers and the advanced MMSE transceivers with various noise levels.

From **Figure 7**, we can see that the advanced MMSE transceiver is better than the iterative MMSE transceiver, especially when we use higher-order PAM. In fact, although the advanced MMSE transceiver is a little complicated than the iterative MMSE transceiver, it is still acceptable because the BER performance has been significantly improved and the indoor VLC system is static in most cases. The optical channel matrix does not change frequently, so the transceivers calculated from our advance MMSE algorithm can be adopted for a long time.

5. Conclusion

In this research, a novel receiver for DCO-OFDM is proposed. The receiver can accurately reconstruct the clipping noise in an iterative manner and then subtract it from the received signal, which can greatly decrease the effects of clipping noise on the system performance. Simulation results showed that the proposed receiver could achieve significant performance gain over the conventional receiver. Based on this, we investigated a MIMO VLC system with illumination control. In contract to radio frequency (RF) systems, VLC systems are limited in dynamic range, which means the transmitter should guarantee that the signal is above the turn-on value l and below the saturation value u of the LED. Under these VLC-specific requirements, we propose an advanced MMSE transceiver based on the iterative MMSE transceiver [14]. From our analysis and simulation, we conclude that the BER performance of our advanced MMSE transceiver is better than the iterative MMSE transceiver in MIMO VLC system when the DC bias is the midpoint of the dynamic range [13].

Acknowledgements

Author details

Jian Dang*, Mengting Wu, Liang Wu and Zaichen Zhang

*Address all correspondence to: newwanda@seu.edu.cn

School of Information Science and Engineering, Southeast University, Nanjing, Peoples Republic of China

References

[1] Wang CX. Cellular architecture and key technologies for 5G wireless communication networks. IEEE Communications Magazine. 2014;**52**(2):122–130. DOI: 10.1109/MCOM.2014.6736752

[2] Komine T, Nakagawa M. Fundamental analysis for visible-light communication system using LED lights. IEEE Transactions on Consumer Electronics. 2004;**50**(1):100–107. DOI: 10.1109/TCE.2004.1277847

[3] Armstrong J. OFDM for optical communications. Journal of Lightwave Technology. 2009;**27**(3):189–204. DOI: 10.1109/JLT.2008.2010061

[4] Armstrong J, Lowery A. Power efficient optical OFDM. Electronics Letters. 2006;**42**(6):370–372. DOI: 10.1049/el:20063636

[5] Mesleh R, Elgala H, Haas H. On the performance of different OFDM based optical wireless communication systems. IEEE/OSA Journal of Optical Communications and Networking. 2011;**3**(8):620–628. DOI: 10.1364/JOCN.3.000620

[6] Armstrong J, Schmidt B. Comparison of asymmetrically clipped optical OFDM and DC-biased optical OFDM in AWGN. IEEE Communications Letters.2008;**12**(5):343–345. DOI: 10.1109/LCOMM.2008.080193

[7] Dimitrov S, Sinanovic S, Haas H. Clipping noise in OFDM-based optical wireless communication systems. IEEE Transactions on Communications. 2012;**60**(4):1072–1081. DOI: 10.1109/TCOMM.2012.022712.100493

[8] Zhang M, Zhang Z. An optimum DC-biasing for DCO-OFDM system. IEEE Communications Letters. 2014;**18**(8):1351–1354. DOI: 10.1109/LCOMM.2014.2331068

[9] Yu Z, Baxley RJ, Zhou GT. EVM and achievable data rate analysis of clipped OFDM signals in visible light communication . EURASIP Journal on Wireless Communications and Networking. 2012;**2012**(321). 1–24. DOI: 10.1186/1687-1499-2012-321

[10] Mesleh R, Mehmood R, Elgala H, Haas H. Indoor MIMO optical wireless communication using spatial modulation. In: IEEE International Conference on Communications; 23-27 May 2010; Cape Town, South Africa. IEEE; 2010. 1–5. DOI: 10.1109/ICC.2010.5502062

[11] Azhar AH, Tran TA, O'Brien D. Demonstration of high-speed data transmission using MIMO-OFDM visible light communications. In: IEEE Globecom Workshop OWC; 6-10 December 2010; Miami, Florida. USA: IEEE; 2011. 1052–1056. DOI: 10.1109/GLOCOMW.2010.5700095

[12] Azhar AH, Tran T-A, O'Brien DC. A gigabit/s indoor wireless transmission using MIMO-OFDM visible-light communications. IEEE Photonics Technology Letters. 2013;**25**(2):171–174. DOI: 10.1109/LPT.2012.2231857

[13] Ying K, Qian H, Baxley RJ, Yao S. Joint optimization of precoder and equalizer in MIMO VLC systems. IEEE Journal on Selected Areas in Communications. 2015;**33**(9):1949–1958. DOI: 10.1109/JSAC.2015.2432515

[14] Ying K, Qian H, Baxley RJ, Tong Zhou G. MIMO transceiver design in dynamic-range-limited VLC systems. IEEE Photonics Technology Letters. 2016;**28**(22):2593–2596. DOI: 10.1109/LPT.2016.2606341

[15] Burton A, Minh HL, Ghassemlooy A, Bentley E, Botella C. Experimental demonstration of 50-Mb/s visible light communications using 4×4 MIMO. IEEE Photonics Technology Letters. 2014;**26**(9):945–948. DOI: 10.1109/LPT.2014.2310638

[16] Thao PC, Khoa DL, Tu NT, Phuc LH, Phuong NH. Optical MIMO DCO-OFDM wireless communication systems using STBC in diffuse fading channels. In: National Foundation for Science and Technology Development Conference on Information and Computer Science; 14-16 September 2016. IEEE; 2016. 141–146. DOI: 10.1109/NICS.2016.7725639

[17] Stepniak G, Siuzdak J, Zwierko P. Compensation of a VLC phosphorescent white LED nonlinearity by means of Volterra DFE. IEEE Photonics Society. 2010;**25**(16):1597–1600. DOI: 10.1109/LPT.2013.2272511

[18] Horn RA, Johnson CR, editors. Topics in Matrix Analysis. New York, USA: Cambridge University Press; 1991. p. 616. DOI: 10.1137/1035037